

1222·2022  
**800**  
ANNI



UNIVERSITÀ  
DEGLI STUDI  
DI PADOVA



# FRAGMENTATION MODELS FOR HYPERVELOCITY IMPACT

Shengyu Zou - 35th Cycle

Supervisor: Prof. Alessandro Francesconi

Presentation for admission to the PhD thesis evaluation procedure– Dec. 15, 2022

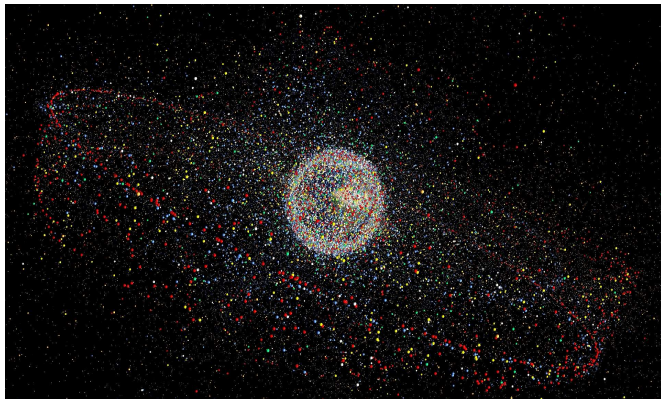
# Outline

- ◆ **Research background and motivations**
- ◆ **Research methodology**
- ◆ **Properties and models for hypervelocity impact fragmentation**
  - Properties and models for debris-cloud velocities
  - Properties and models for perforation hole
  - Properties and models for large central fragment
- ◆ **Experimental research activities**
  - Experimental study on hypervelocity impact debris-cloud
  - Experimental study on backwall damage response
  - Fragments recovery experiment
- ◆ **Conclusions & training activity**

# Research background

## □ Space debris condition

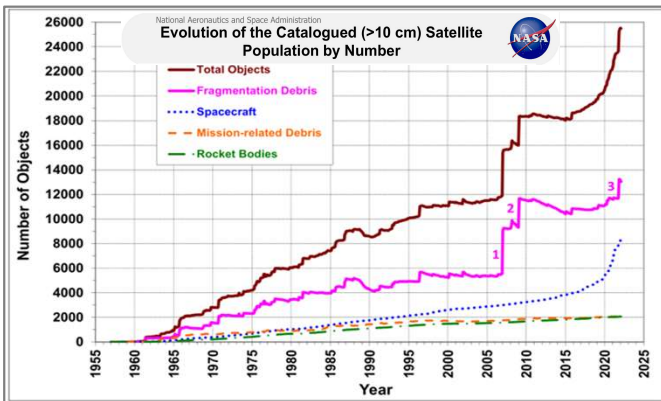
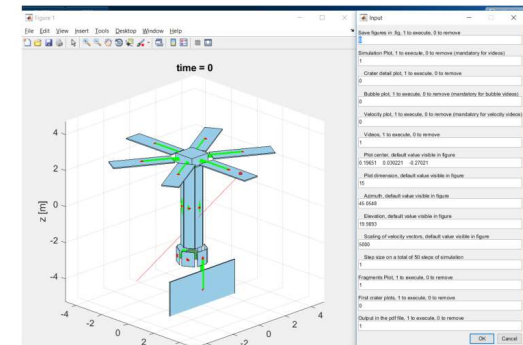
### ➤ Orbital space debris



### ➤ Fragmentation incidents on orbit

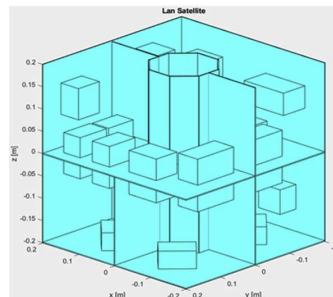


### ➤ Semi-empirical tool in CISAS - CST



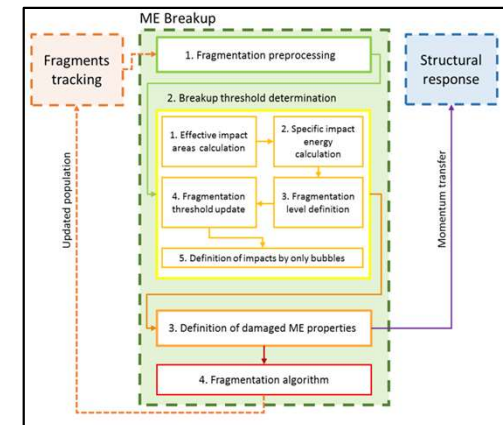
Shengyu Zou

### ➤ Laboratory tests



S. Lan, et al. 2014

FRAGMENTATION MODELS FOR HYPERVELOCITY IMPACT



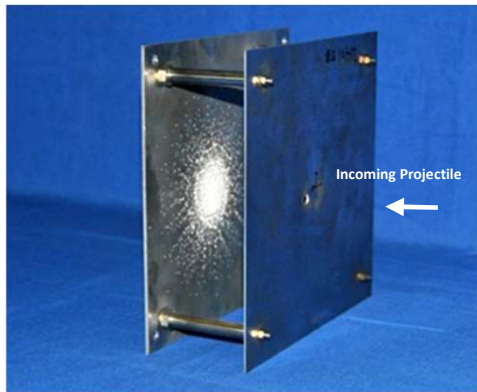
3-25

# Research background

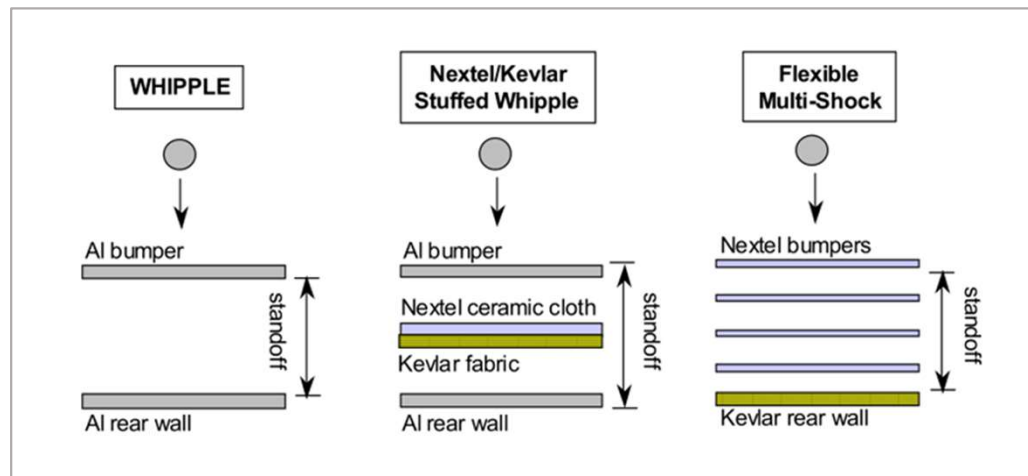
## □ Space debris shields

### ➤ Whipple shield

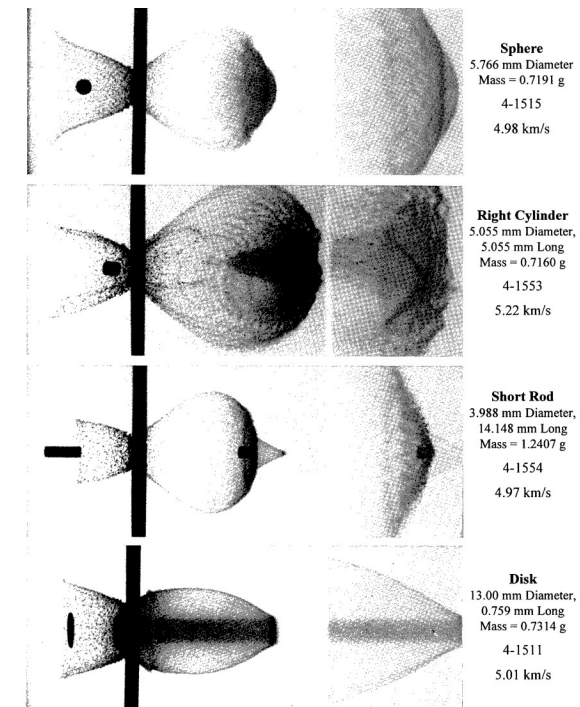
*Whipple F.L in 1947*



### ➤ Stuffed Whipple shields & Multi-shock shields



### ➤ Thin-plate impact & shape effect



*Piekutowski A.J. 1996*

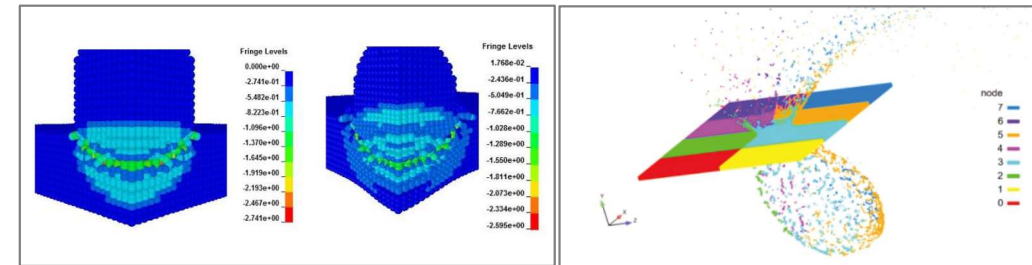
## □ Motivations

- To study the fundamental physics of the hypervelocity impact fragmentation subjected to thin-plate impact, and to characterize the fragmentation properties.
- To develop semi-empirical fragmentation models for hypervelocity impact with consideration of projectile shape effect.

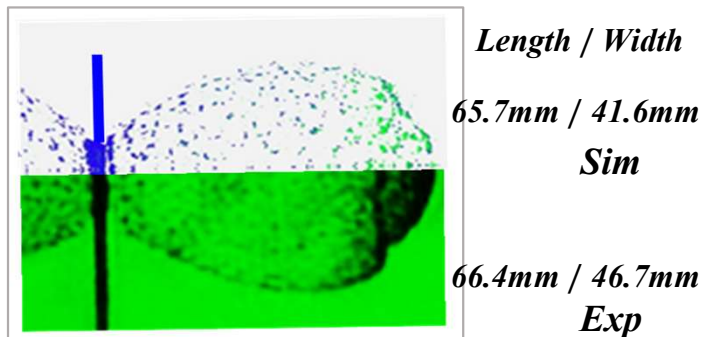


## □ Numerical simulation- Smooth Particles Hydrodynamics (SPH)

- **Meshless method: filling up with particles.**
- **Extreme deformation and high pressure condition.**
- **Parallel SPH code-PTS of HIRC/CARDC**
  - *more efficient & lower occupation of computation resource.*
- **More than 150 simulation cases had been performed in the PhD project.**
- **Validations for simulation model**



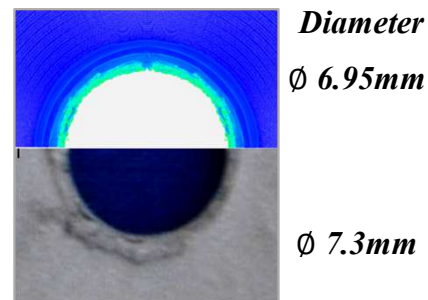
### ✓ Debris cloud



The deviation :

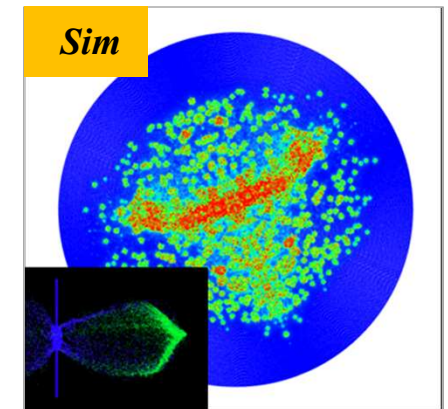
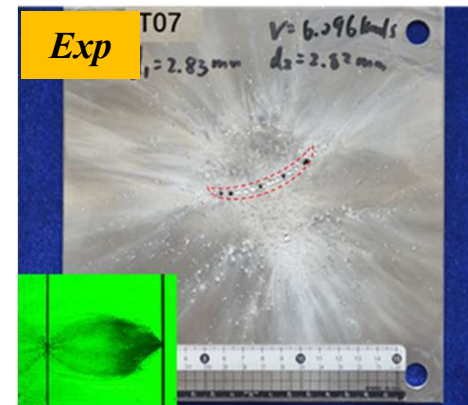
11%

### ✓ Perforation hole



5%

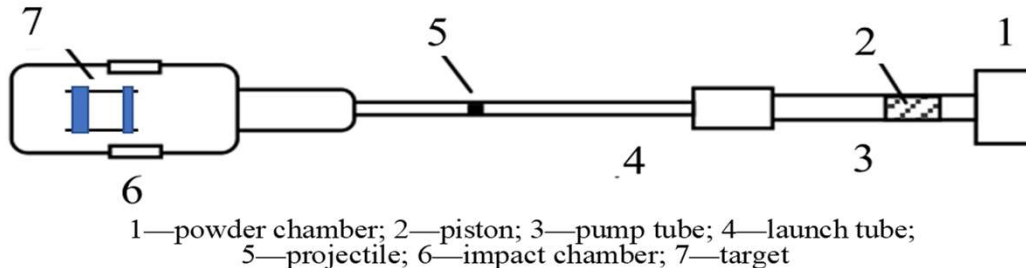
### ✓ Backwall damage



# Research methodology

## □ Hypervelocity impact tests

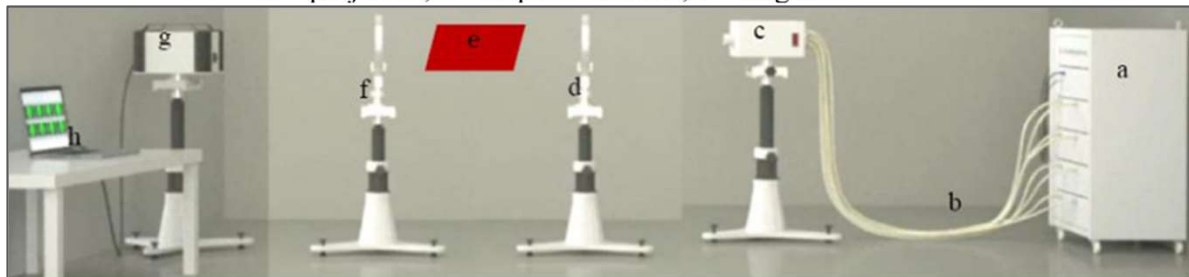
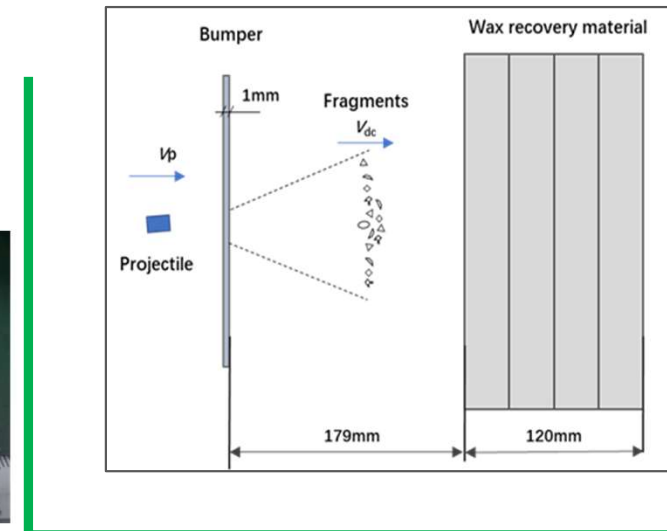
- A total of 20 tests had been performed in the PhD project.
- Test facilities in HIRC:
  - Two-stage-gas-gun, caliber 16mm and 7.6mm, muzzle velocity up to 9km/s.
  - Sequential laser shadowgraph instrument,  $T_{\text{interval}} \geq 10\text{ns}$



### ✓ Projectiles and sabot



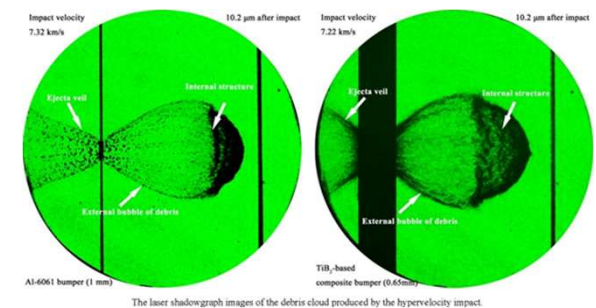
### ➤ Fragments recovery test setup



a—pulsed lasers; b—optical fiber; c—light-separating instrument; d—collimating len-1;  
e—measuring area; f—collimating len-2; g—image system; h—control system

Shengyu Zou

### ✓ Debris cloud of impact at above 7km/s



FRAGMENTATION MODELS FOR HYPERVELOCITY IMPACT

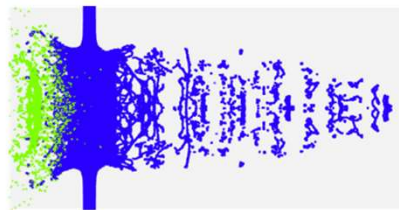
# Properties and models for debris-cloud velocities

## □ Study on debris cloud geometry

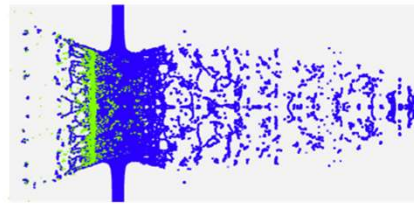
➤ For the case of 7km/s to 2mm bumper

  
 Projectile material

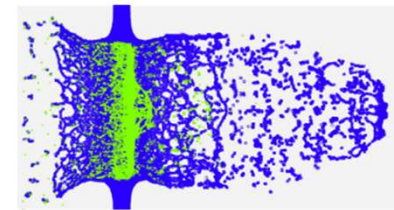
  
 Bumper material



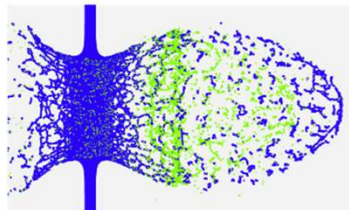
$L/d=0.05$



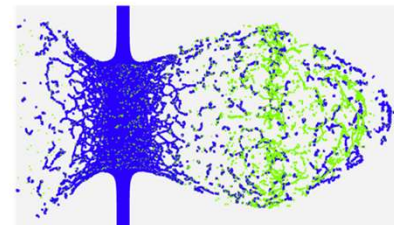
$L/d=0.1$



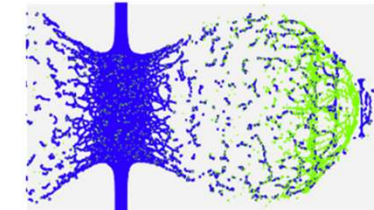
$L/d=0.2$



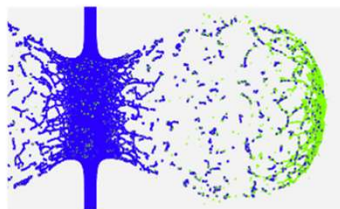
$L/d=0.5$



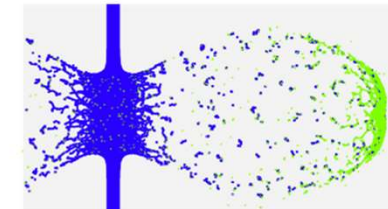
$L/d=0.75$



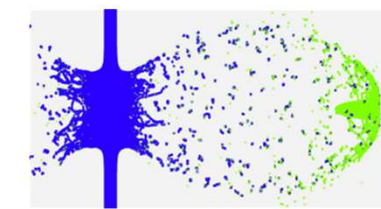
$L/d=1.0$



$L/d=1.5$



$L/d=3.0$



$L/d=5.0$

- Flat disk-like projectile produces a columnar debris cloud, in which the projectile material falls far behind the bumper material.

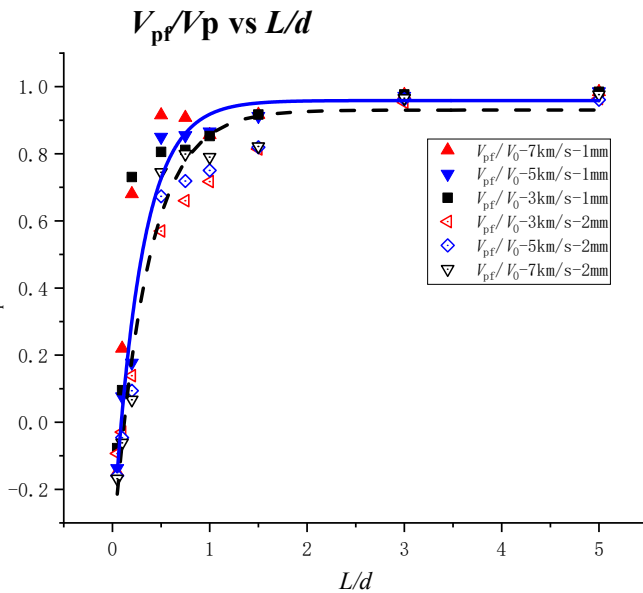
- Spherical projectile produces a more expanding debris cloud similar to spherical shell, in which the projectile material is located at the front part.

- Rod-like projectile produces a elliptical debris cloud, in which large remain of projectile is located at the leading part.

# Properties and models for debris-cloud velocities

## Characterization of debris cloud velocities

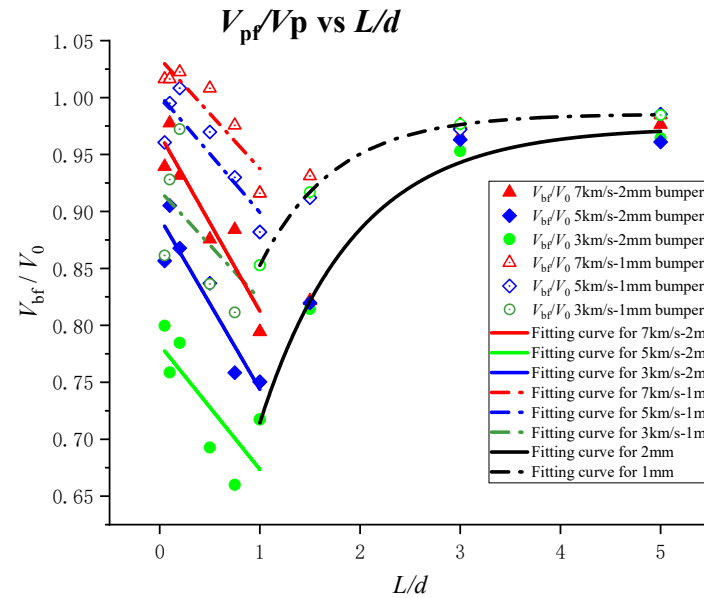
### ➤ Projectile front velocity



- Disk-like projectile: lower or backward axial moving velocity.
- Sphere and rod-like projectile: higher projectile fragments velocity.
- Thicker sheet : little effect on the projectile leading-edge velocity.
- Nearly linear relationship between  $V_{pf}$  and  $V_0$ .

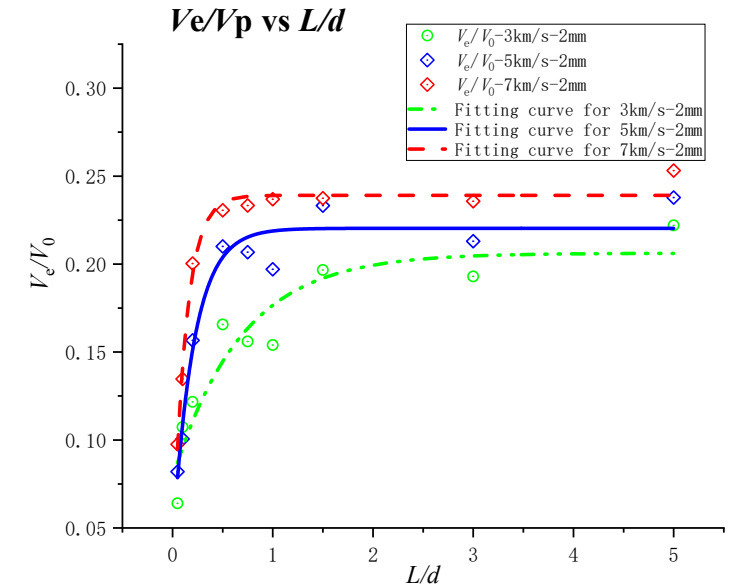
Shengyu Zou

### ➤ Bumper front velocity



- Sphere-like projectile: lower velocity of  $V_{bf}$ .
- Disk-like and rod-like projectile: higher velocity of  $V_{bf}$ .
- Linear relationship between  $V_{bf}/V_0$  and  $L/d$  where  $L/d < 1$ .
- Exponential relationship between  $V_{bf}/V_0$  and  $L/d$  where  $L/d \geq 1$ .

### ➤ Expanding velocity



- Disk-like projectile: lower expanding velocity.
- Sphere and rod-like projectile: higher expanding velocity.
- Thicker sheet : lower expanding velocity.
- Nonlinear relationship between  $V_e$  and  $V_0$ .

Ref: S. Zou, L. Olivieri a, Z. Ma c, C. Giacomuzzo a,b, A. Francesconi. 72nd IAC, Oct. 2021.

FRAGMENTATION MODELS FOR HYPERVELOCITY IMPACT

8-25



# Properties and models for debris-cloud velocities

## Models for Debris-cloud velocities

### ➤ Semi-empirical dimensionless model

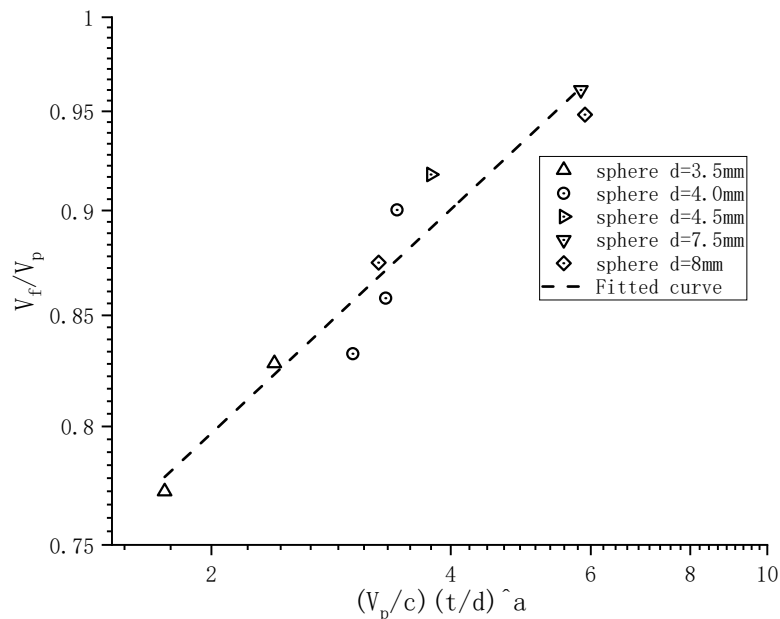
$$\frac{V_{dc}}{V_p} = C \cdot \left(\frac{t}{d}\right)^a \cdot \left(\frac{V}{c}\right)^\beta \cdot \left(\frac{L}{d}\right)^\gamma$$

### ➤ Calibration and validation with test data

### ✓ *Calibrated parameters table*

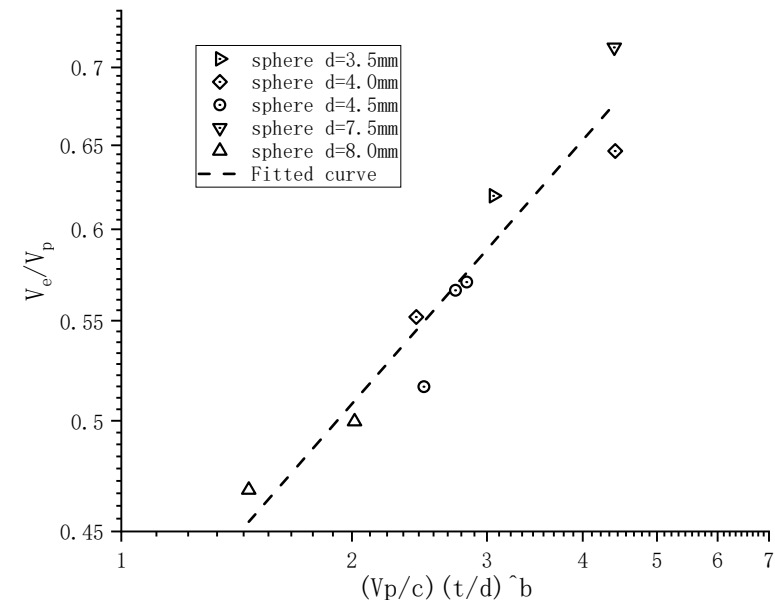
Parameters	Model for $V_f$	Model for $V_e$
$C$	0.7053	0.3953
$\alpha$	0.1761	0.3623
$\beta$	-0.1391	-0.2355

### ✓ *Validation for front velocity of spherical impact*



Shengyu Zou

### ✓ *Validation for expanding velocity of spherical impact*



FRAGMENTATION MODELS FOR HYPERVELOCITY IMPACT

9-25

# Properties and models for perforation hole

## Models for perforation hole

Maiden CJ, McMillan  
AR. AIAA 1964;2(11).

$$\frac{D_h}{d} = 2.4 \cdot \frac{V_0}{c} \cdot \left(\frac{t}{d}\right)^{2/3} + 0.9$$

Shape effect  
consideration  $f(L/d)$



**Model-1:**  $\frac{D_h}{d} = 2.4 \cdot \frac{V_0}{c} \cdot \left(\frac{t}{d}\right)^{2/3} \cdot f\left(\frac{L}{d}\right) + 0.9$

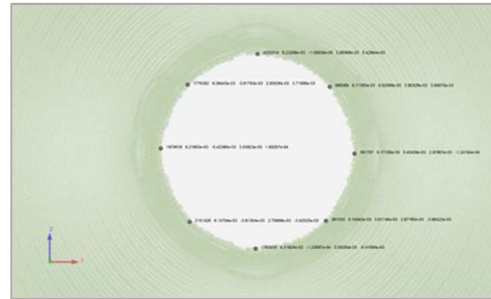
Where  $f\left(\frac{L}{d}\right) = k_1 \left(\frac{L}{d}\right)^a \cdot e^{k_2 \frac{L}{d}}$

**Model-2:**  $\frac{D_h}{d} = 2.4 \cdot \left(\frac{v}{c}\right) \cdot \left(\frac{t}{d}\right)^{f_2(L/d)} \cdot f_1\left(\frac{L}{d}\right) + 0.9$

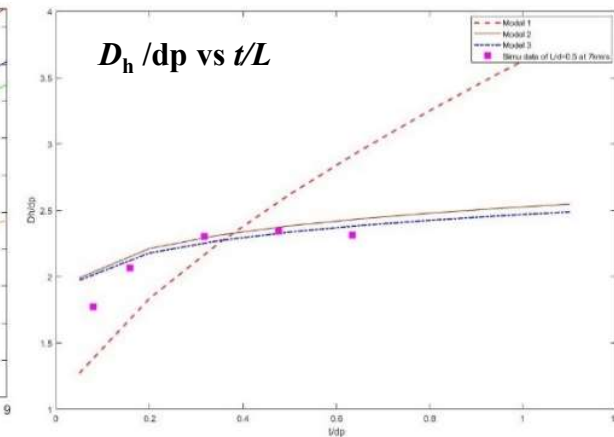
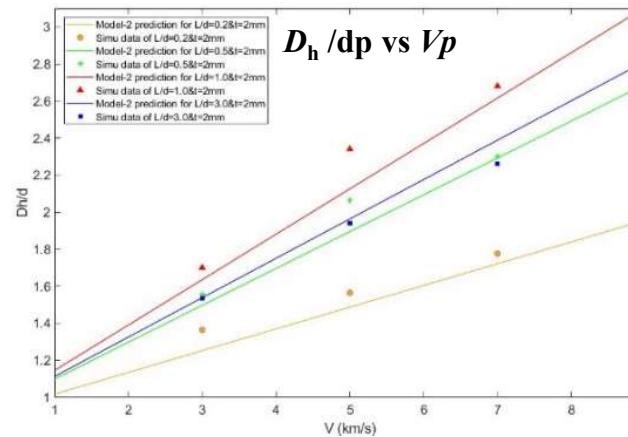
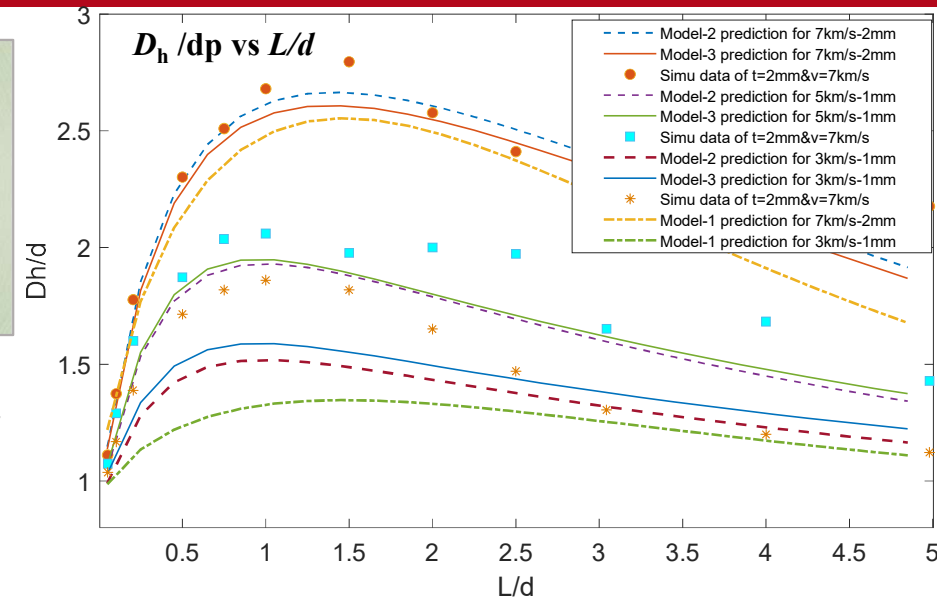
Where  $f_1\left(\frac{L}{d}\right) = q_1 \left(\frac{L}{d}\right)^{q_2} \cdot e^{q_3 \frac{L}{d}}$

$f_2\left(\frac{L}{d}\right) = \left(\frac{L}{d}\right)^{p_1} + p_2 e^{p_3 \frac{L}{d}}$

**Model-3:**  $\frac{D_h}{d} = k_1 \cdot \left(\frac{V_0}{c}\right)^{w_1} \cdot \left(\frac{t}{d}\right)^{w_2} + w_3 e^{w_4 \frac{L}{d}} \cdot \left(\frac{L}{d}\right)^{w_5} \cdot e^{w_6 \frac{L}{d}} + k_2$



✓ Comparisons and  
Validation



Ref: S. Zou, L. Olivieri a, Z. Ma c, C. Giacomuzzo a,b, A. Francesconi. 72nd IAC, Oct. 2021.

Shengyu Zou

FRAGMENTATION MODELS FOR HYPERVELOCITY IMPACT

10-25

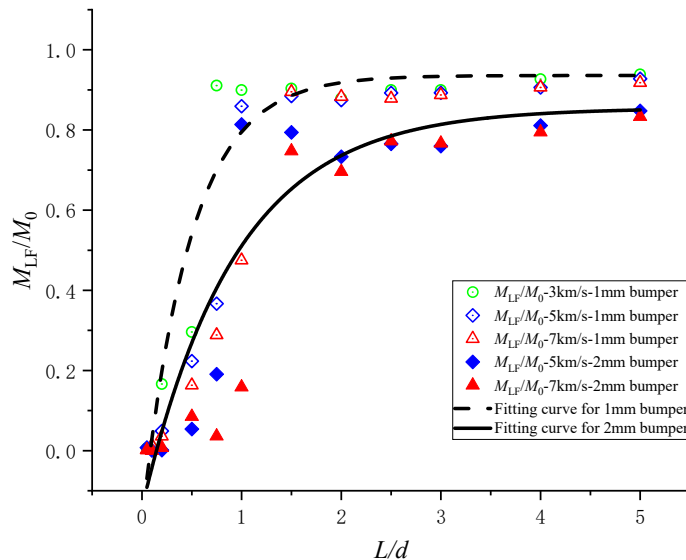
# Properties and models for large central fragment

## □ The effect of projectile shape $L/d$

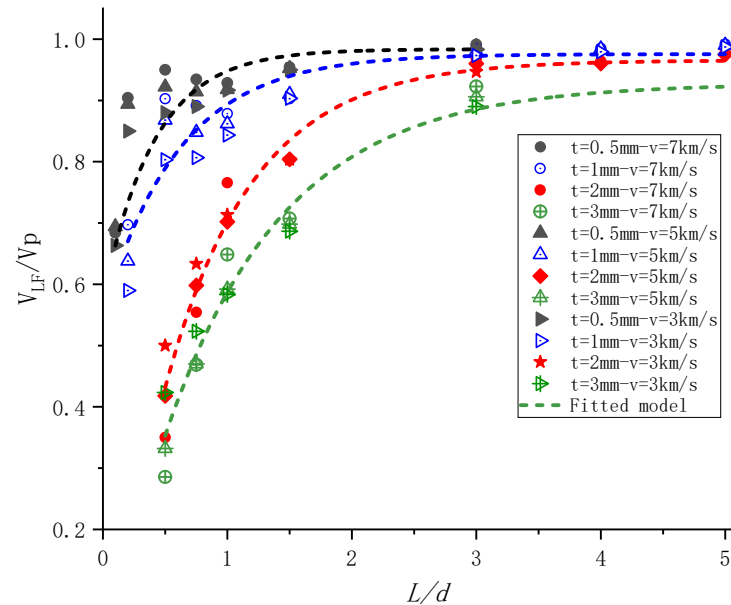
$M_{LF}$  was normalized by dividing it by the projectile mass  $M_p$ .

$V_{LF}$  was normalized by dividing it by the impact velocity  $V_p$ .

$M_{LF}/M_p$  vs  $L/d$



$V_{LF}/V_p$  vs  $L/d$



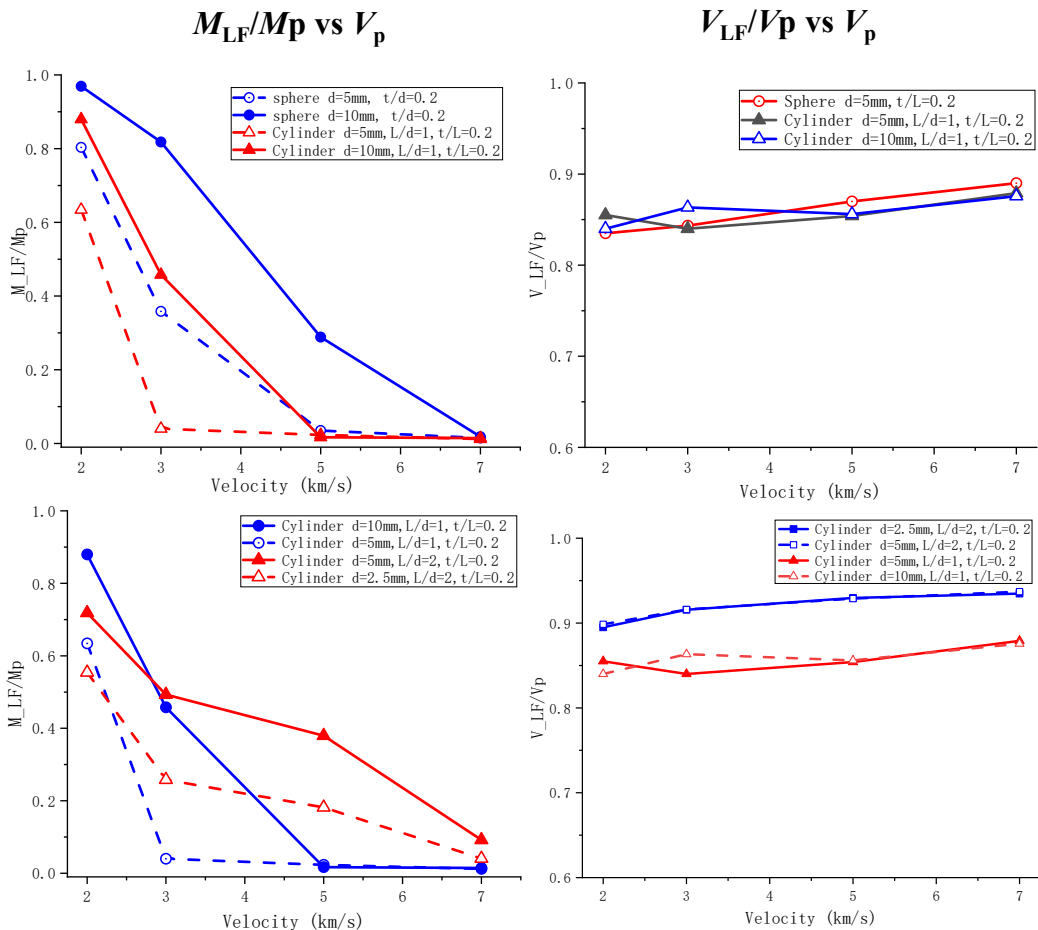
•  $M_{LF}$  is dependent on projectile shape, target thickness and impact velocity, while  $V_{LF}$  appears to depend on projectile shape and target thickness, but only slightly depend on impact velocity.

• Disk-like projectiles ( $L/d \ll 1$ ) are easiest to be fragmented, and have relative lower velocity of the large fragment.

• Rod-like projectiles are usually less fragmented and less impeded by thin plate target during hypervelocity impacts.

# Properties and models for large central fragment

## □ The effect of impact velocity



Shengyu Zou

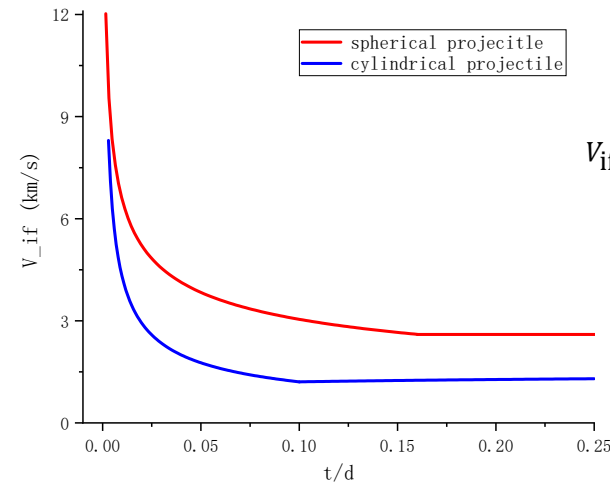
## ➤ Geometrical scaling investigation

- $V_{LF}$  is geometrical scaling for both spherical and non-spherical projectiles, while  $M_{LF}$  is not geometrical scaling but is size-dependent.

$$\frac{M_{LF}}{M_p} \propto \left(\frac{L}{d}\right)^\alpha \cdot \left(\frac{t}{L}\right)^\beta \cdot f\left(C \frac{V_p}{d}\right)$$

$$\frac{V_{LF}}{V_p} \propto C \cdot \left(\frac{L}{d}\right)^a \cdot \left(\frac{t}{L}\right)^b \cdot \left(\frac{V_p}{c}\right)^\gamma$$

## ➤ Fragmentation threshold-velocity investigation



✓ **For sphere**

$$V_{if} = \begin{cases} 1.436 \text{ km/s} \cdot \left(\frac{t}{d}\right)^{-0.333} & \text{for } \frac{t}{d} < 0.16 \\ 2.6 \text{ km/s} & \text{for } \frac{t}{d} \geq 0.16 \end{cases}$$

✓ **For short-cylinder**

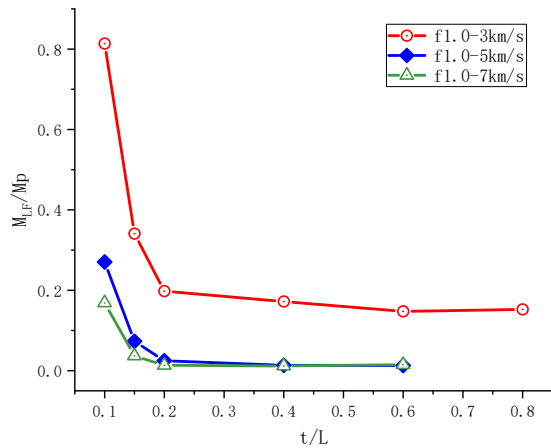
$$V_{if} = \begin{cases} 0.34 \text{ km/s} \cdot \left(\frac{t}{d}\right)^{-0.55} & \text{for } \frac{t}{d} \leq 0.1 \\ 1.45 \text{ km/s} \cdot \left(\frac{t}{d}\right)^{0.08} & \text{for } \frac{t}{d} > 0.1 \end{cases}$$



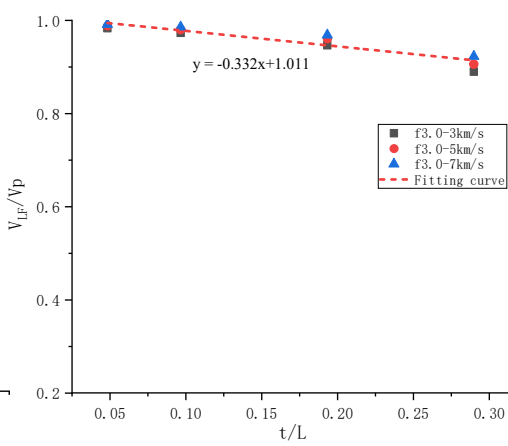
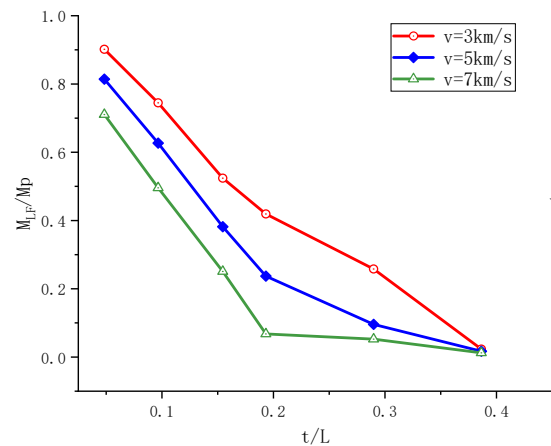
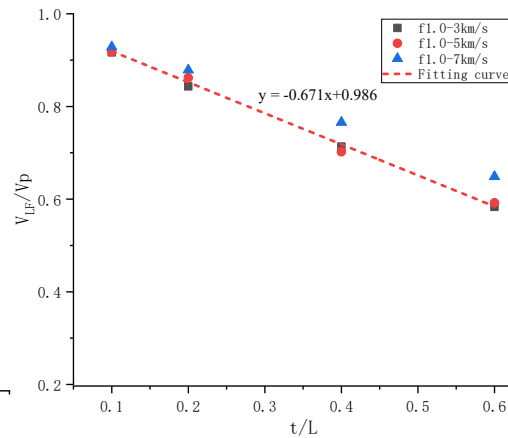
# Properties and models for large central fragment

## □ The effect of target thickness ratio $t/L$

$M_{LF}/M_p$  vs  $t/L$

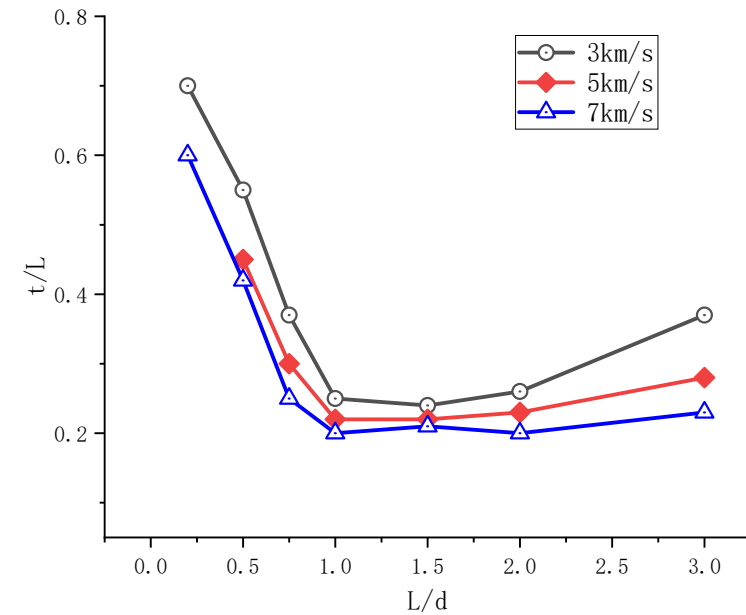


$V_{LF}/V_p$  vs  $t/L$



## ➤ Investigation on optimum bumper-thickness-ratio

- a sphere and a short-cylinder ( $L/d > 1$ ) have a lower optimum  $t/L$  ratio than a disk-like projectile ( $L/d < 1$ ) with equivalent initial mass.
- for designing a more conservative shield, it is necessary to carry out the evaluation tests by using disk-like projectiles rather than spheres or short cylinders.



# Properties and models for large central fragment

## □ Dimensional analysis for modelling

Based on Pi theorem, three fundamental variables: mass ( $\hat{M}$ ), length ( $\hat{L}$ ), time ( $\hat{T}$ ).

✓ *The units and dimensions of the variables*

Variables	Units	Dimensions
t, L, d	m	$\hat{L}$
$V_p, V_{if}, c$	m/s	$\hat{L} \cdot \hat{T}^{-1}$
$M_p, M_{LF}$	kg	$\hat{M}$
$\rho_p$	kg/m <sup>3</sup>	$\hat{M} \cdot \hat{L}^{-3}$
$\gamma$	N/m <sup>2</sup>	$\hat{M} \cdot \hat{L}^{-1} \cdot \hat{T}^{-2}$
$K_c$	N/m <sup>3/2</sup>	$\hat{M} \cdot \hat{L}^{-1/2} \cdot \hat{T}^{-2}$

### ➤ The mass of the large central fragment

$$M_{LF} = f(t, L, d, V_p, S, Z_p/Z_t)$$

Nondimensionalization

$$\frac{M_{LF} \cdot \rho_p \cdot V_p^{2-y}}{\rho_p L d^2 \cdot S \cdot d^{-x-y}} = f\left(\frac{t}{L}, \frac{L}{d}, \frac{Z_p}{Z_t}\right)$$

$$\frac{M_{LF}}{M_p} = \frac{S \cdot d^{-x-y}}{\rho_p \cdot V_p^{2-y}} \cdot f\left(\frac{t}{L}, \frac{L}{d}, \frac{Z_p}{Z_t}\right) \quad \frac{M_{LF}}{M_p} = C \cdot d^{-x-y} \cdot V_p^{-2+y} \cdot \left(\frac{t}{L}\right)^\alpha \cdot \left(\frac{L}{d}\right)^\beta$$

The model for large-central-fragment mass

$$1 - \frac{M_{LF}}{M_p} = \begin{cases} \approx 0 & \text{for } V_p \leq V_{if} \\ C d^\omega \left(\frac{V_p - V_{if}}{V_{if}}\right)^\alpha \left(\frac{t}{d}\right)^\beta \left(\frac{L}{d}\right)^\gamma & \text{for } V_{if} \leq V_p \leq V_{cf} \\ \approx 1 & \text{for } V_p > V_{cf} \end{cases}$$

Shengyu Zou

### ➤ The velocity of the large central fragment

$$V_F = f(t, d, L, K)$$

Nondimensionalization

$$\frac{V_F \cdot K}{d^{1+x}} = f\left(\frac{t}{L}, \frac{L}{d}\right)$$

$$V_F = C \cdot d^{1+x} \cdot \left(\frac{t}{L}\right)^\alpha \cdot \left(\frac{L}{d}\right)^\beta \quad \rightarrow \quad \frac{V_F}{V_p} = C \cdot \left(\frac{t}{L}\right)^\alpha \cdot \left(\frac{L}{d}\right)^\beta \cdot \left(\frac{V_p}{c}\right)^\gamma$$

The model for large-central-fragment velocity

# Properties and models for large central fragment

## □ The model for large-central-fragment mass

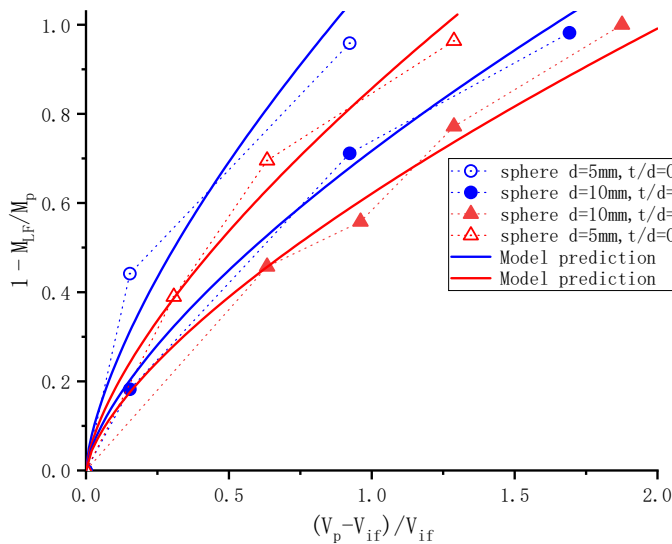
### ➤ Model formulation

$$1 - \frac{M_{LF}}{M_p} = \begin{cases} \approx 0 & \text{for } V_p \leq V_{if} \\ C d^\omega \left( \frac{V_p - V_{if}}{V_{if}} \right)^\alpha \left( \frac{t}{d} \right)^\beta \left( \frac{L}{d} \right)^\gamma & \text{for } V_{if} \leq V_p \leq V_{cf} \\ \approx 1 & \text{for } V_p > V_{cf} \end{cases}$$

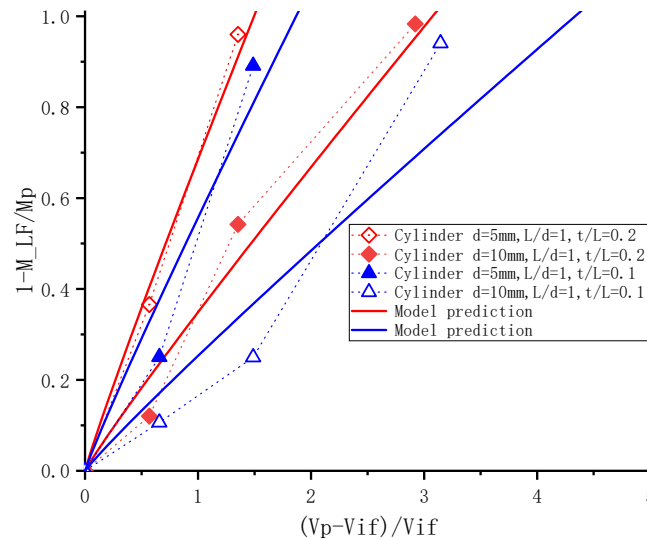
### ➤ Calibration and validation

### ✓ Calibrated parameters table

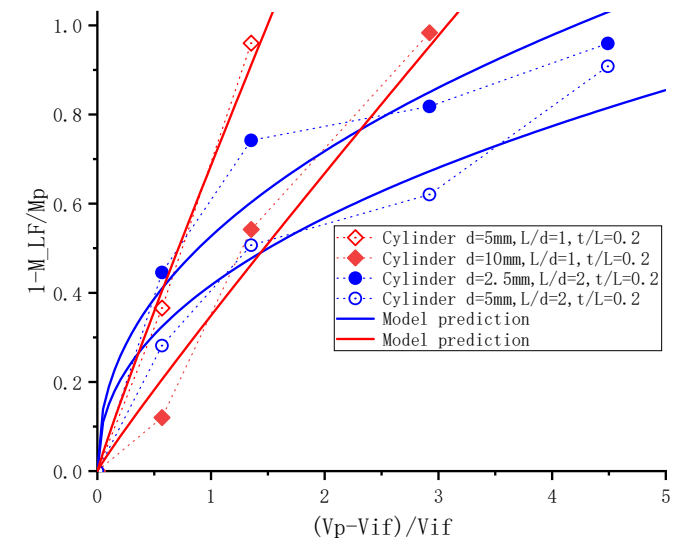
Parameters	Projectile type		
	Sphere	Cylinder-L/d=1	Cylinder-L/d=2
C	4.471 mm <sup>0.561</sup>	4.072 mm <sup>0.794</sup>	4.072 mm <sup>0.794</sup>
ω	-0.561	-0.794	-0.794
α	0.675	0.937	0.577
β	0.316	0.331	0.331
γ	0	-1.003	-1.003



Shengyu Zou



FRAGMENTATION MODELS FOR HYPERVELOCITY IMPACT



15-25

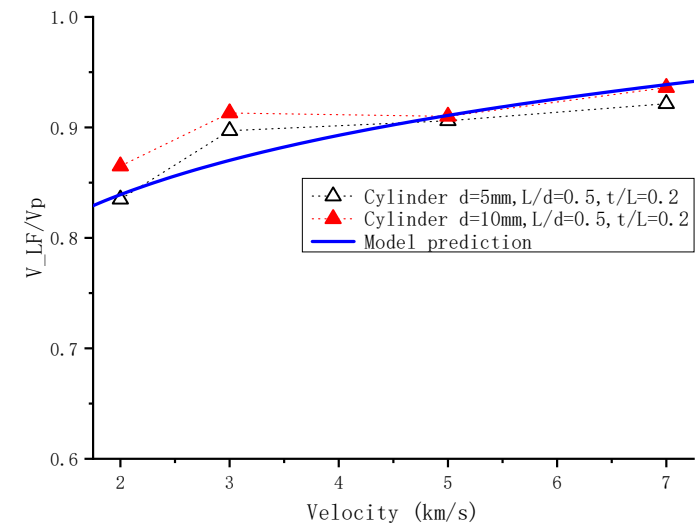
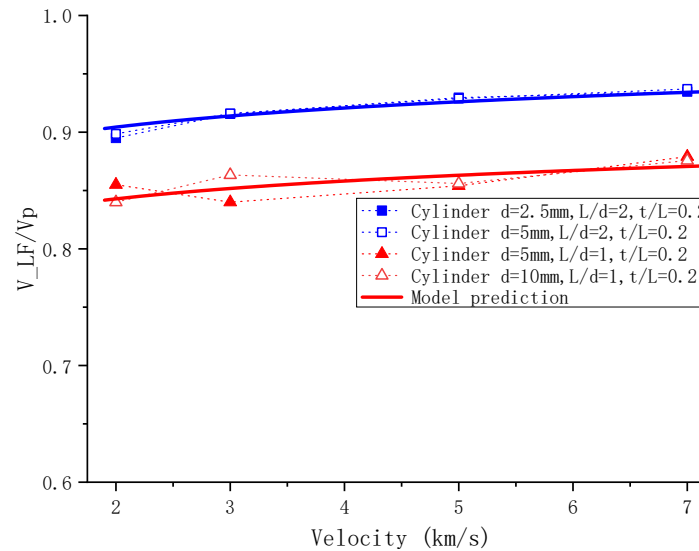
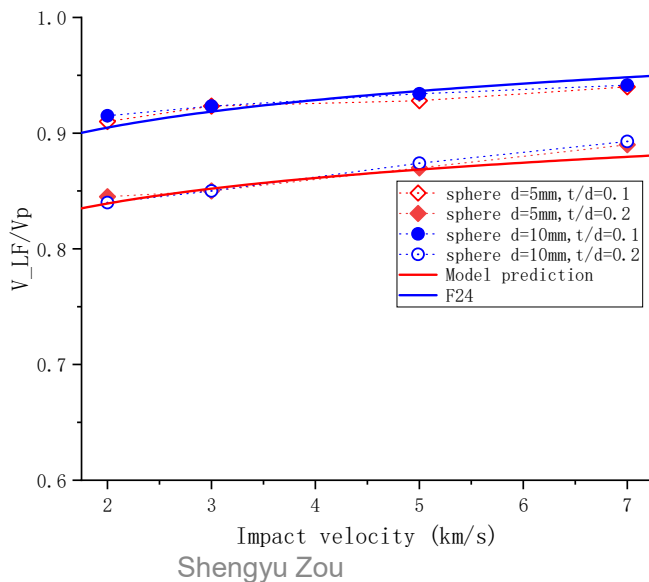
# Properties and models for large central fragment

## □ The model for large-central-fragment velocity

### ➤ Model formulation

$$\frac{V_{LF}}{V_p} = C' \cdot \left(\frac{V_p}{c_t}\right)^{\alpha'} \cdot \left(\frac{t}{L}\right)^{\beta'} \cdot \left(\frac{L}{d}\right)^{\gamma'}$$

### ➤ Calibration and validation



### ✓ Calibrated parameters table

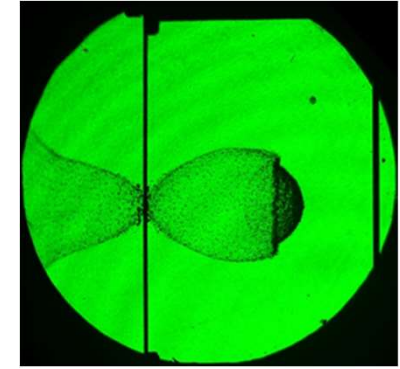
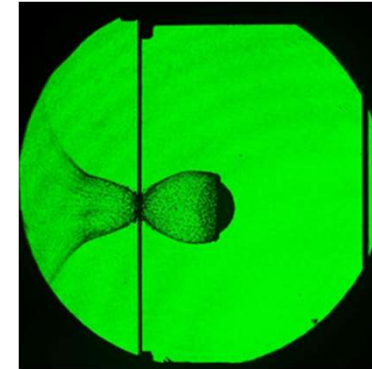
Parameters	Projectile type		
	Sphere	Cylinder or ellipsoid	
		L/d=0.2~0.75	L/d=1~2
$C'$	0.7306	0.7338	0.7202
$\alpha'$	0.0375	0.0895	0.0259
$\beta'$	-0.1086	-0.1080	-0.1132
$\gamma'$	0	-0.0671	0.1016



## □ Debris cloud morphology

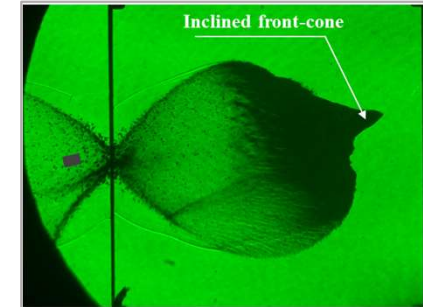
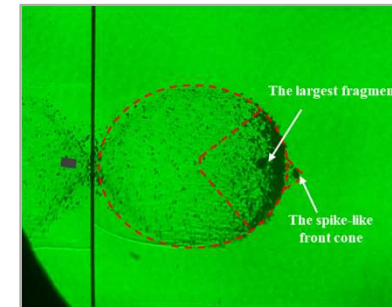
### ➤ Sphere impact

- an external bubble and an internal structure including front cap, central element and rear element.
- a hemispherical shell of fragments spalling off the rear side of the projectile .



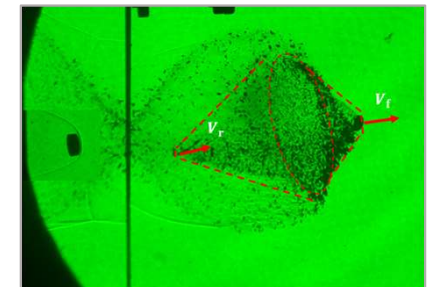
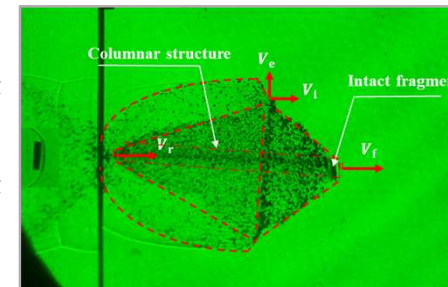
### ➤ Short-cylinder impact

- a spike-like front cone at the leading edge with velocity of up to 4% greater than impact velocity.
- the head point of the front cone is coincident with the direction of the cylinder axis, and is dependent on the cylinder's impact inclination.



### ➤ Disk impact

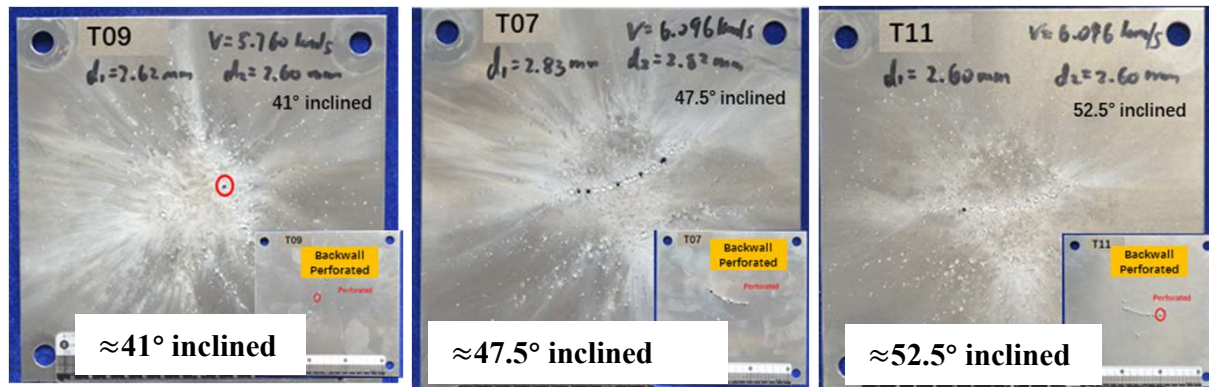
- consist of an external bubble, an internal cone and a front cone with its point aligned with the inclined direction of the disk axis.
- there is a long columnar structure in the middle, a fast-moving head at about 3% higher than  $V_p$ , and a very slow-moving end at only 6% of  $V_p$ .
- the columnar structure doesn't show any tendency to disperse.



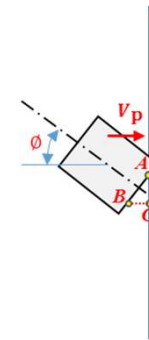
# Experimental study on backwall damage response

## □ The inclination effect on backwall damage

### ✓ Backwall images from experiments



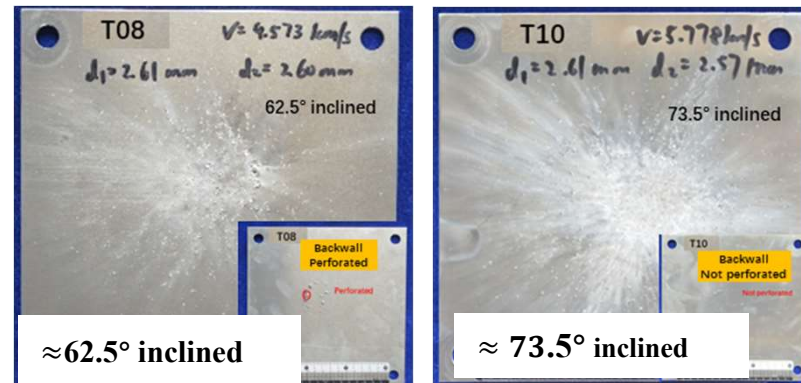
### ✓ Analytic model for critical inclined angel



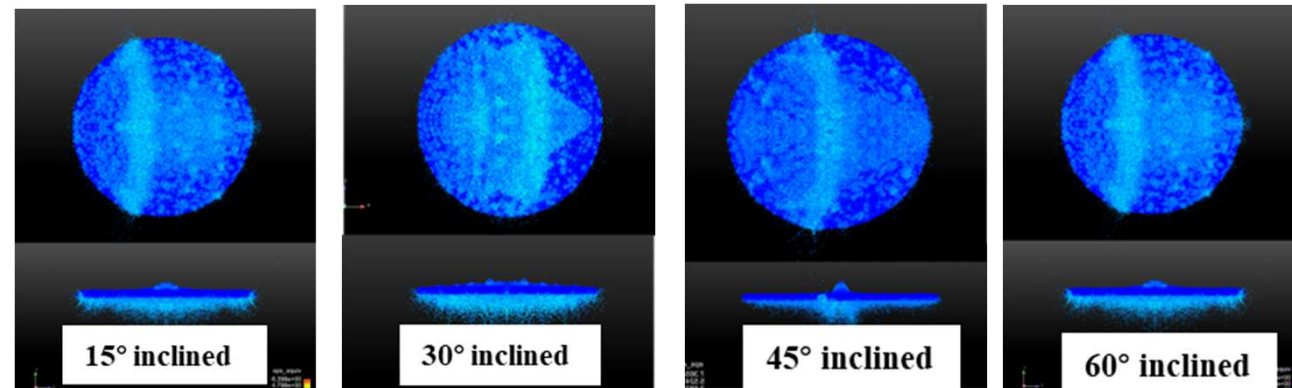
$$\sin \phi_{cr} = \frac{BC}{AB} = \frac{v_p}{U_s}$$

$$U_s = c_t + \frac{kv_p}{2}$$

- For Al-Al impact at about 6km/s, it is more damaging situation when the inclination is between  $40^\circ$  to  $50^\circ$



### ✓ Backwall images from simulations



FRAGMENTATION MODELS FOR HYPERVELOCITY IMPACT

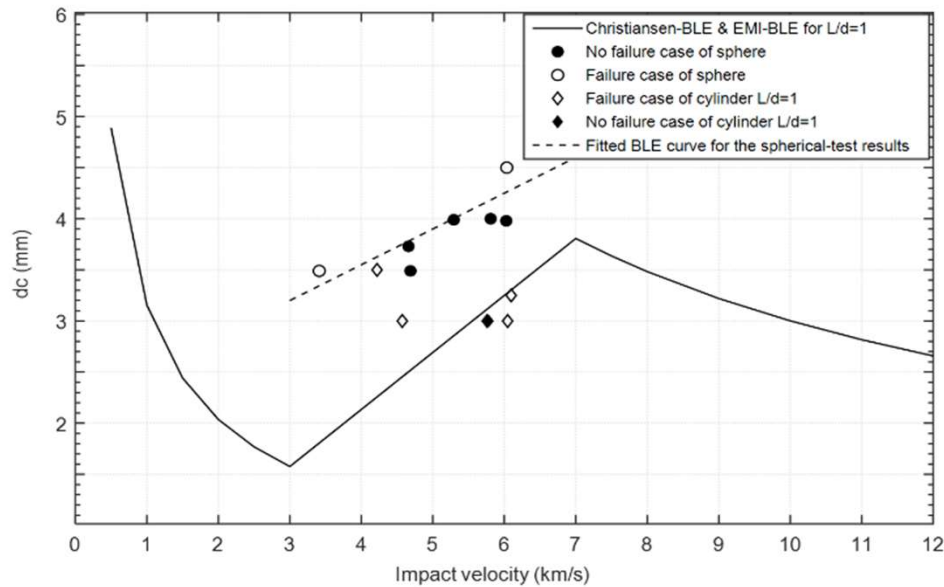
18-25

# Experimental study on backwall damage response

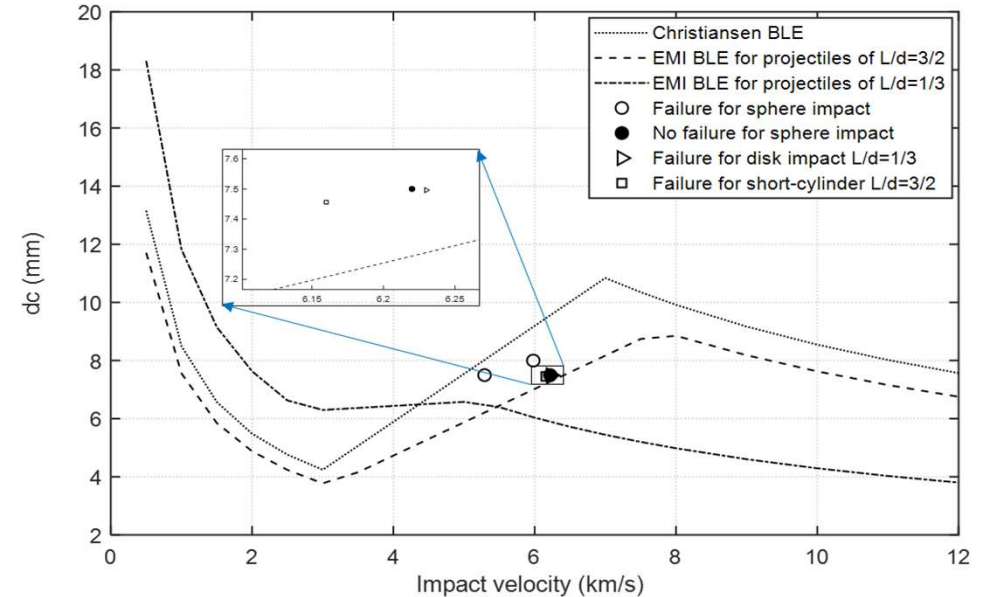
## □ Ballistic limit equation for Whipple shields

Examination and comparison of two BLE models: Christ-BLE and EMI-BLE.

**WS-1:  $t_b$ -S- $t_w$ : 1mm-80mm-2mm**



**WS-2:  $t_b$ -S- $t_w$ : 1mm-129mm-7mm**



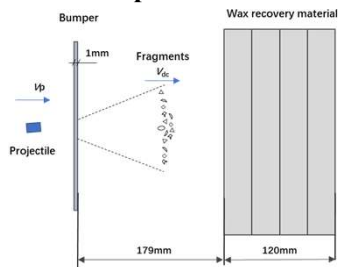
- Christ-BLE is up to 2 times more conservative for evaluating the performance of spherical impact against WS-1, but it is dangerous when used for non-spherical impact.
- EMI-BLE is much more conservative than Christ-BLE, and could be applied for non-spherical impacts.
- Both of the two BLEs could not be applied conservatively for the impacts with inclined cylinder.



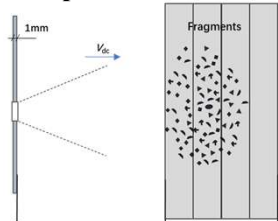
# Fragments recovery experiment

## □ Fragments recovery and analysis

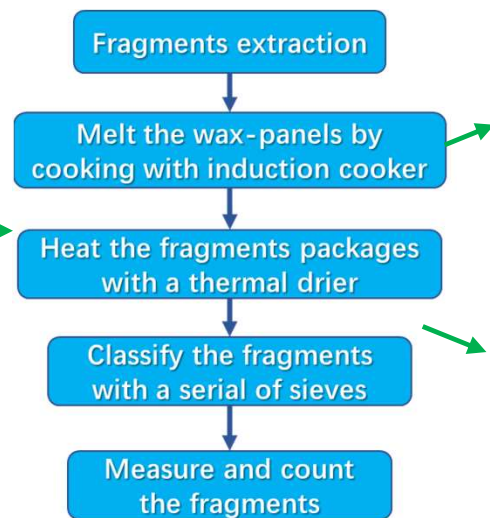
### ✓ Before the impact



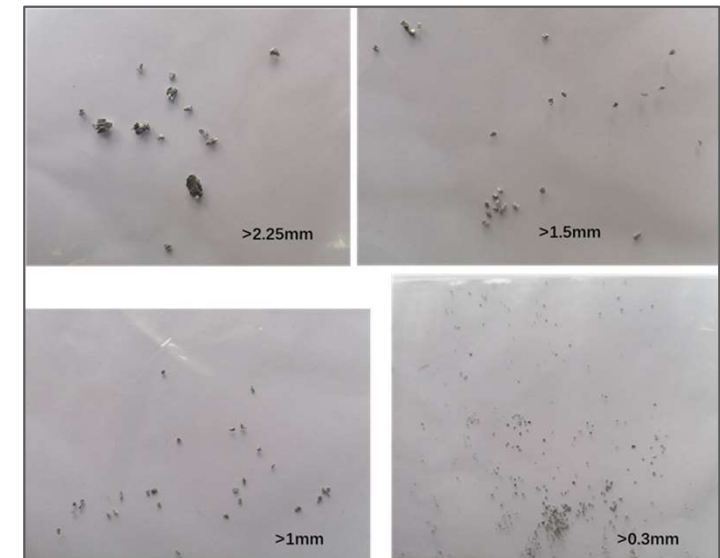
### ✓ After the impact



### ✓ Fragments recovery procedures



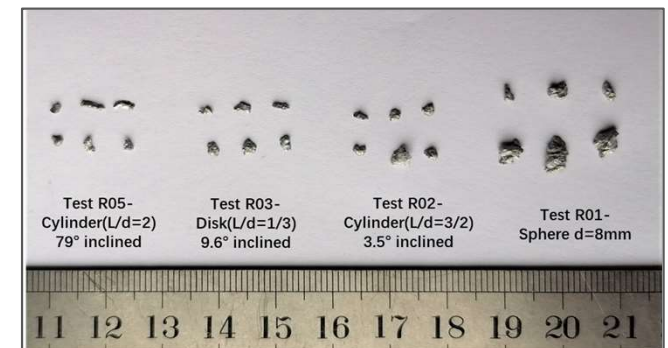
### ✓ Fragments collected from spherical impact



## Comparisons of large fragments for impacts with different shaped projectiles

- The disk-like projectile is easiest to be fragmented, sphere is harder to be fragmented than short-cylinder .
- Impact of short-cylinder with large inclination undergoes a complete fragmentation like a disk projectile .

Shengyu Zou



FRAGMENTATION MODELS FOR HYPERVELOCITY IMPACT

20-25



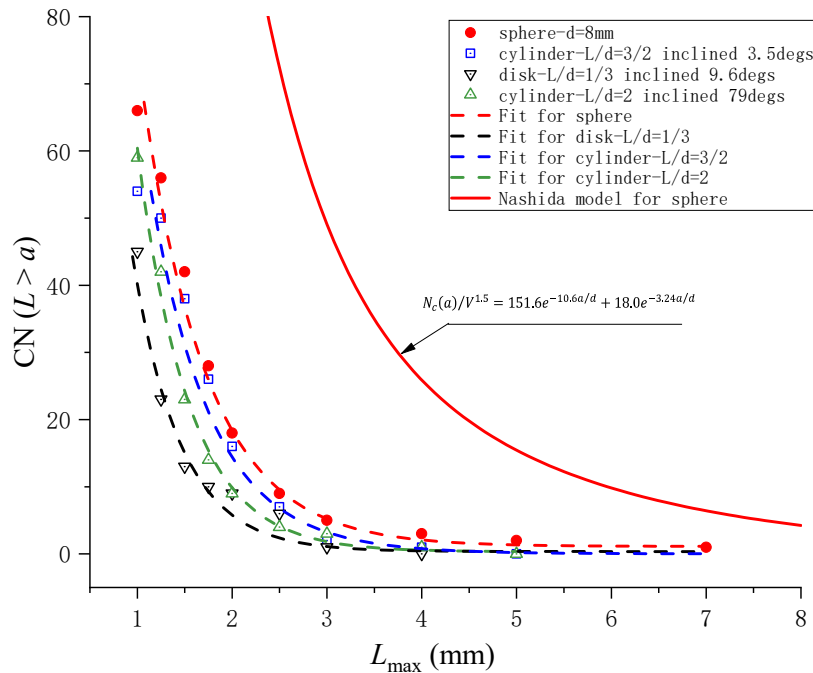
## □ Fragments distribution and model

### ➤ For sphere impact

#### Nashida Model:

*M. Nishida, et al. 1917*

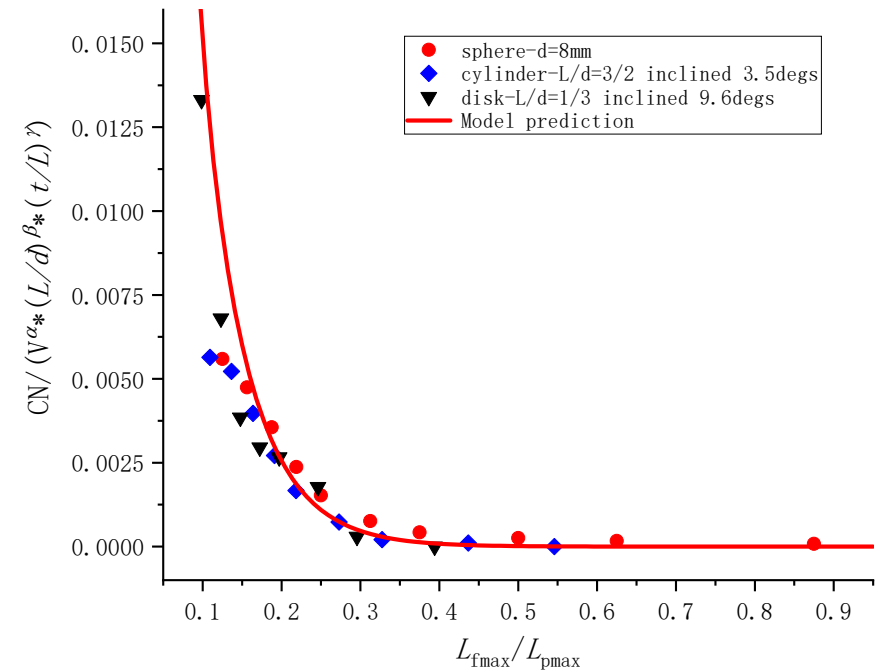
$$N_c(a)/V^{1.5} = 50.7e^{-1.6a/d} + 2.9e^{-4.3a/d}$$



### ➤ A scaling model developed for impact with shaped projectiles

$$\frac{N_c(a)}{V_p^\alpha \cdot (t/L)^\beta \cdot (L/d)^\gamma} = A_1 e^{B_1 a/L_{pmax}} + A_2 e^{B_2 a/L_{pmax}}$$

Parameters	$\alpha$	$\beta$	$\gamma$	$A_1$	$B_1$	$A_2$	$B_2$
Values	1.5	-3.65	-1.75	1.332	-70.657	0.076	-16.975



# Conclusions & training activity

- **Characterizing projectile shape effect on debris cloud geometry and debris cloud motions:**
  - Flat disk-like projectile produces debris cloud with columnar geometry, in which the expansion velocity of debris cloud is lower, while the leading-edge velocity is relatively higher; the debris cloud produced by a sphere-like projectile has a higher expansion velocity but a lower leading-edge velocity, that means the debris cloud has a higher level of fragments diffusion; the fragmentation rate caused by impacting with a rod-like projectile is significantly insufficient, thus the total fragments population is significantly small, and the debris cloud includes a primary fragment with both mass and velocity close to those of projectile before collision.
- **Properties study and model development for debris-cloud velocities:**
  - Debris cloud structure for different projectile shape were studied from the debris-cloud morphology based on simulation and experiments. The debris-cloud velocities were characterized and semi-empirical models for spherical impact have been developed.
- **Properties study and model development for perforation hole :**
  - Based on simulation data, the sphere or short-cylinder is strongest in the enlargement capability of the perforation hole, while the rod-like projectile takes lower capability, and the flat disk-like projectile takes the lowest capability. Three semi-empirical models were proposed and compared.
- **Properties study and model development for large central fragment:**
  - The effects of shape ratio, target thickness ratio and impact velocity on the mass and the velocity of large central fragment were characterized, and semi-empirical models for the mass and the velocity of large central fragment were developed based on dimensional analysis, and were calibrated and validated with simulation data.

# Conclusions & training activity

- **Investigated on fragmentation threshold velocity :**
  - There existed two threshold-velocities for judging the fragmentation intensity, one is the threshold-velocity of initiation fragmentation  $V_{if}$ , and another is the threshold-velocity of catastrophic fragmentation  $V_{cf}$ . Disk-like projectile has the lowest fragmentation threshold velocity, rod-like projectile has the largest fragmentation threshold velocity, and sphere or short-cylinder have moderate fragmentation threshold velocity. Short cylinder can be fragmented more easily than sphere at fixed  $t/d$  ratio.
- **Investigated on optimum bumper-to-projectile thickness ratio:**
  - A sphere and a short-cylinder ( $L/d > 1$ ) have a lower optimum  $t/L$  ratio than a disk-like projectile ( $L/d < 1$ ). Such that it appears to be not conservative when sphere or short-cylinder is used to evaluate the effectiveness of a shield against space debris impacts. Thus for designing a more conservative shield, it is necessary to carry out the evaluation tests by using disk-like projectiles rather than spheres or short cylinders.
- **Investigated on geometrical scaling of large-central-fragment:**
  - The velocity of the large central fragment is geometrical scaling for both spherical and non-spherical projectiles, while the mass of the large central fragment is not geometrical scaling but is size-dependent.
- **Investigated on the inclination effect on cylindrical impact :**
  - The work of simulation, experiment and analytic model had performed. The investigation indicates: for inclined impact, the most damaged area on rear wall was commonly crescent-shaped, and biased away the central craters. For Al-to-Al impact, there is a more damaging situation when the inclination is between  $40^\circ$  to  $50^\circ$ .

# Conclusions & training activity

- Investigated on BLE models for damage evaluation:
  - Christ-BLE is up to 2 times more conservative in spherical impact for evaluating the performance Whipple shield-1 employed in our tests, but it is dangerous when used for non-spherical impact. Another observation is that Christ-BLE is not applicable for evaluating the shielding configuration with lower t/d ratio under the impact velocity higher than 6km/s; It is observed that it is rather conservative with respect to Christ-BLE, and it is applicable for evaluating the non-spherical impacts against Whipple shield-2, but it is not applicable for an inclined impact of right-cylinder.
- Investigated on fragments distribution:
  - The projectile shape as well as the impact inclination are effective on fragments distribution. The mass of the largest-fragment for the spherical impact is 4 times larger than that of the short-cylinder ( $L/d=3/2$ ) impact, and is 10 times larger than that of the disk ( $L/d=1/3$ ). This indicates the disk-like projectile is easiest to be fragmented, and a short-cylinder is easier to be fragmented than a sphere. An scaling model on the fragments distribution has been developed.
- Educational activities during PhD study:

EDUCATIONAL ACTIVITIES ACTIVATED BY THE STMS PHD COURSE								
Interdisciplinary	Module/Activity	Lecturer	Expected credits	Frequency (YES/NO)	Exam (YES/NO) *	Date of exam	Attained credits	
	Space optics and detectors	Prof. G.Naletto	4	YES	YES	03-04-2020	4	
	Exploring the solar system and its environment	Prof. M.-G.Pelizzo Prof. G.Cremonese Prof. F.Marzari	4	YES	YES	26-06-2020	4	
	Mechanical and thermal properties of material for aerospace constructions	Prof. U.Galvanetto Prof. M.Zaccariotto Prof. A.Francesconi	4	YES	No exam	—	4	
	Space systems and their control	Prof. E.Lorenzini	4	YES	YES	28-07-2020	4	
	Measurement techniques: fundamentals, PC based, visual and thermal	Prof. M.Pertile	4	YES	NO	—	0.8	
	Image analysis based	Prof. G.Rossi	2	YES	—	—	0.4	
	Writing a Scientific Paper / Research Project Proposal	Prof. G.Naletto	2	YES	—	—	2.0	
	Introduction to Computational Fluid Dynamics	Prof. F.Picano	3	YES	No exam	—	0.6	
	Composite materials: Modeling, Processing, and Characterization (AIDAA Course)	Prof. M. Petrolo	1	YES	No exam	—	0.2	
	An overview on space debris protection best practices (AIDAA Course)	Post Dr. L. Oliveri	1.5	YES	No exam	—	0.3	
	Structure dynamics: theory and practices in the space industry (AIDAA Course)	Prof. G. Aglietti et al	2.0	YES	YES	04-05-2020	2.0	
	Remote sensing instruments for atmospheric transparency: theory, instruments and methods	Prof. Doro - Gaug	2.0	YES	YES	—	2.0	
	Durability and Ageing Organic Matrix Composites for Aircraft Applications	Prof. Marco Gigliotti	0.78	YES	YES	01-07-2020	0.78	
	Safety course: GENERAL HEALTH AND SAFETY IN THE WORKPLACE	E-learning and Online test		YES	Partly yes	—		
	PhD English course	Prof. Gillian davis		YES	Exam	—		
Curriculum oriented seminars			Lecturer	Expected credits	Frequency (YES/NO)	Exam (YES/NO) *	Date of exam	Attained credits
	Introduction to Quantum Technologies	Prof. Vallone	0.08	YES	NO	25-02-2020	0.08	
	Analysis of Complex Dynamics with Chaos Indicators	Prof. Guzzo	0.08	YES	NO	—	0.08	
	VUV optical anisotropy of few layers graphene: possible application for space	Prof. Zuppella	0.4	YES	YES	29-05-2020	0.4	
	FLY-Spec: UV-VIS-NIR reflectometry and laser-induced breakdown Spectroscopy							
	Advanced Computational Modeling of Multiphase	Prof. F. Picano	0.4	YES	YES	11-6-2020	0.4	
	From Art to Science: The Flower Constellations	Prof. Mortari	0.04	YES	NO	28-01-2021	0.04	
	Computational modelling of strain localisation and crack initiation and propagation in multi-phase porous materials	Prof. L. Sanavia	0.4	YES	YES	01-02-2021	0.4	
	Space electric propulsion	Prof. Magarotto	0.08	YES	YES	18-6-2021	0.08	
	Characterisation of fracture resistance of interfaces in mode I, mode II and mixed mode	Prof. G. Alfano	0.08	YES	-	19-01-2022	0.08	
	Recent advances in numerical approach for multiphase flows	Prof. P. S. Costa Prof. F. Picano	0.08	YES	-	21-02-2022	0.08	
	Computational approaches for fluid-structure interaction with fracturing	Prof. F. D. Barba	0.08	YES	-	21-02-2022	0.08	
	Very low Earth Orbit Satellites for Earth Observations	Prof. F. Barato	0.4	YES	YES	21-02-2022	0.4	
	Operating a detector in space for 10 years: the case of Fermi LAT course	Prof. R. Rando	0.4	YES	YES	24-02-2022	0.4	
	Past and future imaging of the surface of Mars	Prof. N. Thomas	0.08	YES	-	09-03-2022	0.08	
	Dispersed Multiphase Flows: Physics and Modelling	Prof. F. Picano	0.08	YES	-	22-03-2022	0.08	
	Tethers for space applications: current developments and future perspectives	Prof. E. Lorenzini	0.08	YES	—	27-04-2022	0.08	
	The OSIRIS-REx sample return mission: a journey to the origin of the Solar System	Prof. M. Pajola	0.4	YES	YES	09-05-2022	0.4	
OTHER EDUCATIONAL ACTIVITIES								
Title of the activity (Date/Period/University)	Lecturer	Duration of activity	Expected credits	Frequency (YES/NO)	Exam (YES/NO)	Date of exam	Attained credits	
Admission presentation	YES		0.5	YES	NO	21-02-2020	0.5	
First year admission presentation	YES		0.5	YES	YES	06-11-2020	0.5	
Second year admission presentation	YES		0.5	YES	YES	11-01-2022	0.5	
Third year admission presentation	YES		0.5	YES	YES	15-12-2022	0.5	
Dissertation defense presentation	YES		0.5					
Conferences 1 time: International Astronautics Congress 2021	YES		1.0	YES	YES		1.0	
Total of expected ECTS credits attainable in educational activities (>30):			31.74	Total of credits attained in educational activities (at date 15 Dec. 2022):			31.24	

# Thanks for your attention

1222 · 2022  
**800**  
ANNI



UNIVERSITÀ  
DEGLI STUDI  
DI PADOVA

